Surface Glass Transition Temperature of Amorphous Polymers. A New Insight with SFM

ARTICLE *in* MACROMOLECULES · JULY 2002

Impact Factor: 5.8 · DOI: 10.1021/ma011326a

3 AUTHORS, INCLUDING:

Hazel E. Assender
University of Oxford
86 PUBLICATIONS **1,207** CITATIONS
SEE PROFILE

George Andrew D Briggs
University of Oxford
473 PUBLICATIONS **11,770** CITATIONS
SEE PROFILE

Article

Surface Glass Transition Temperature of Amorphous Polymers. A New Insight with SFM

V. N. Bliznyuk, H. E. Assender, and G. A. D. Briggs

Macromolecules, **2002**, 35 (17), 6613-6622• DOI: 10.1021/ma011326a • Publication Date (Web): 18 July 2002

Surface Glass Transition Temperature of Amorphous Polymers. A New Insight with SFM

V. N. Bliznyuk,† H. E. Assender, and G. A. D. Briggs*

Department of Materials, Oxford University, Oxford OX1 3PH, UK

Received July 25, 2001; Revised Manuscript Received March 28, 2002

ABSTRACT: The surface glass transition temperature, T_g, of several amorphous polystyrene (PS) samples each with a narrow molecular weight distribution covering the range of M_n from 3 900 to 1 340 000 has been measured by force−distance measurements using a scanning force microscope (SFM). Hysteresis in the loading−unloading cycles of the force−distance curves is observed above T_g and is ascribed to viscoelasticity at the polymer surface. The hysteresis behavior for different molecular weight samples above T_g is described in terms of the contact mechanics of the tip−surface interaction, by consideration of the relative roles of bulk viscoelasticity and peeling viscoelasticity. Data on the molecular mass dependence of thick films of the surface T_g are presented, along with the dependence of T_g on film thickness for thin films, and the annealing of films with a Langmuir−Blodgett overlayer. The results are related to existing theories describing the T_g depression at lower M_n as a result of the increased free volume in the system. The change in T_g with molecular weight of PS is steeper for the surface than the bulk Fox−Flory relationship. We show that polymer chain entanglement variation rather than the end group localization on the free surface is responsible for the observed surface T_g depression effect.

Introduction

During past decade there has been a burst of publications in the field of polymer science of nanocomposites. Some such composites are layered structures where the polymer serves as a substrate for further deposition of thin layers.[1,2] Knowledge of the surface properties of polymer films in comparison to their bulk analogues may be a crucial factor in the achievement of better physical parameters of such composites.

The glass transition temperature (T_g) is one of the most important parameters characterizing a polymer compound as an engineering material. The Young's modulus, for instance, decreases 3 orders of around T_g for many polymers.[3,4] It has been demonstrated that the T_g of ultrathin films, confined geometries, and surfaces can differ by as much as several tens of degrees from corresponding bulk values.[5−12] The magnitude of the effect is still a matter of investigation, with some studies (e.g., refs 13 and 14) showing no enhanced mobility near the surface and others (e.g., refs 15−18) showing a difference from bulk behavior only for certain ranges of molecular weight. There are three important factors that must be carefully considered when comparing these experimental data: the geometry of the sample, the molecular weight of the polymer, and the nature of what is probed by the experimental technique. We will discuss each of these briefly in turn.

The geometry of the sample will control the nature and degree of confinement of the molecules that is thought to control the relaxation behavior close to the surface. This "confinement" of the chains near a surface has two aspects: that due to the topology of the system in which the conformation of the molecules near the surface is modified in order to define the surface plane and the confinement of the molecular motions due to free volume and interaction effects with the surface. Three major geometries have been studied: (i) thin free-standing films in which the molecules are conformationally confined within a thin layer, but there is reduced hindrance compared with the bulk polymer to molecular motions on both sides of the film; (ii) thin films on an (often strongly) adhering surface in which the molecules are conformationally confined to the layer on both sides and there is only one "free" surface where there is reduced hindrance to molecular motion (and such motion may more restricted on the adhering surface); and (iii) the surface of "bulk" films—a semi-infinite layer in which the molecules are not geometrically confined in the direction into the film (i.e., they tend to a bulklike conformation in this direction), and there is reduced hindrance to molecular motion, compared with the bulk polymer on the free surface only. For the case of artificially roughened surfaces,[11] there is additionally some lateral chain confinement within the topography of the free surface but enhanced "free surface" area for more chain motion.

The issue of molecular weight dependence has been shown to be coupled to this geometric effect,[16] where for free-standing films the greatest molecular weight dependence has been shown for high molecular weights, in contrast to the results from thin supported films. The authors suggest that the alternative "sliding motion" relaxation mode proposed by de Gennes[19] is prevented by chain confinement in supported films but, where two free surfaces are present, can account for the observed molecular weight dependence for the longer molecules. At low molecular weights, whole chain dynamics dominate in free-standing films, hence showing little molecular weight dependence. Where the molecular motions are more confined in supported films, segmental motion must dominate, and there is once more a molecular weight dependence at low molecular weights. The case of a free surface on a bulk polymer film will be different again but is generally shown to behave more like a layer that is confined on the bottom surface, due to the

† Present address: CMD Department, Western Michigan University, Kalamazoo, MI 49008.

10.1021/ma011326a CCC: $22.00
Published on Web 07/18/2002

penetration of surface molecules into the more bulklike material beneath. Hence, the T_g depression is often observed for low molecular weights.[15,17,18]

Finally, care must be taken in determining the particular molecular relaxations probed in any particular experiment. One might envisage a range of processes of different nature: the fast motion associated with local rearrangements (attempted conformational changes), a slower motion due to the cooperative motion of molecular segments, and slow reptation or flow of the polymer chain. The experimental technique used to probe the "glass transition" will reflect different proportions of these motions, and in some cases, the dynamical processes involved are difficult to isolate. For example, lateral force microscopy and SFM lateral force modulation mode experiments have been carried out by several groups, and the type of relaxation process probed by such experiments should be taken into account. Kajiyama et al.[9] performed a thorough study of PS surface thermomechanical properties with a high-frequency (15 kHz) modulation scanning technique (scanning viscoelastic microscopy). Their interpretation of the results of the tip−surface interaction indicated a dependence of the surface glass transition temperature on molecular mass, which was much stronger than the dependence for bulk polystyrene. More recent results[10] using lateral force microscopy on PS with specific end groups found a relationship $T_{g0} \propto M_n^{-0.6}$ and a depression in surface T_g even to very high molecular weights, indicating that surface segregation of end groups cannot completely account for the surface T_g dependence. Rather, the authors invoked a contribution from shorter-range relaxation effects appropriate to the greater deformation rates of this technique. On the other hand, Overney et al. have been using almost the same experimental technique and found no sign of the surface glass transition depression.[14] Moreover, their results demonstrated the dependence of the effective transition temperature measured at the surface on the scanning parameters (such as scanning rate and normal load applied to the surface), therefore illustrating possibilities for artifacts in T_{g0} estimation from scanned measurements.[20] This mode of measurement involves a more complex interaction between a scanned tip and the sample than our force−distance measurements, and their results illustrate the necessity to consider carefully the nature of the deformation and peeling effects of the material on this very small scale when measuring T_g. Similarly, surface relaxation in PS was studied by fine structure (NEXAFS) experiments.[13] No evidence of enhanced mobility at the free surface was found. However, the authors distinguished two types of polymer chain mobility (and two characteristic length scales): the relaxation of the polymer within the first nanometer of the surface, parallel to the surface (i.e., two-dimensional), whereas within the first 10 nm depth from the surface the dominant relaxation occurred normal to the free surface. The observed discrepancy with previous optical experiments could be naturally explained as a result of probing the different processes. Relatively slow relaxation of the polymer chain, which depends critically on chain conformations near the polymer/air interface (distribution of entanglements and chain ends), may be available in experiments measuring thermal expansion or mechanical characteristics along the normal to the surface.[15]

Table 1. Structural Characteristics of Amorphous PS Samples[a]

M_n	polydispersity index M_w/M_n	R_g [nm]
3 900	1.11	1.7
9 300	1.13	2.6
20 800	1.07	4.0
34 000	1.06	5.1
115 900	1.04	9.3
347 000	1.06	16.2
965 000	1.15	27.0
1 340 000	1.05	31.8

[a] The radius of gyration is calculated using a random coil approximation with monomer size $a = 0.254$ nm and free volume parameter $C_\infty = 9$.[28]

The scanning force microscopy (SFM) technique is a sensitive tool for the study of the surface elastic and adhesion interaction properties[21,22] and is extremely suitable for addressing polymer chain surface dynamics, i.e., testing of T_g properties of a polymer surface region on a bulklike polymer material. The method has been developed into a family of techniques allowing simultaneous investigation of not only structure with nanometer scale resolution but also mechanical and thermodynamic properties on the surface.[22,23]

In this paper we present our measurements of the surface glass transition temperature on a set of polystyrene (PS) fractions with a narrow molecular mass distribution by SFM force−distance mode experiments. The T_g is measured as a function of the molecular mass and analyzed in terms of two models of chain mobility over a depth comparable with the polymer chain dimensions: (a) that determined by chain end segregation and (b) that determined by the entanglement of polymer chains.

Experimental Section

A Park Scientific Instruments Autoprobe CP atomic force microscope operated in contact mode has been employed for these experiments. Si_3N_4 cantilevers with a spring constant of 0.26−0.40 N m^{-1} and a characteristic tip radius of curvature ~10 nm were chosen for force−distance measurements near the glass transition, where the mechanical properties such as stiffness are expected to change from a gigapascal to several megapascal range.[24] The polymer surface morphology was studied in noncontact mode at room temperature. Mechanical properties of the surface were measured in force−distance mode in the temperature range 20−170 °C. A miniature heater that allows SFM experiments to be carried out at elevated temperatures was constructed.[27] A two-step calibration procedure was applied to achieve surface temperature control. The heater was first calibrated with a nickel−chromium/nickel−aluminum thermocouple firmly attached (glued) to the surface. The calibration curve (either temperature vs applied voltage or temperature vs current) so obtained was linear in the range of temperatures 50−180 °C. The heater calibration was also checked and corrected under experimental conditions from the melting points of a Wood alloy with $T_m = 70$ °C, In/Sn (52/48) alloy ($T_m = 118$ °C), and indium ($T_m = 156.6$ °C). A precision in the surface temperature measurement of ±3 °C has been achieved.

A set of narrow molecular weight distribution fractions of polystyrene (Polymer Source Inc., Canada) with molecular weights ranging from 3.9×10^3 to 1.34×10^6 g mol^{-1} has been studied. This molecular weight range covers almost 2 orders of magnitude in characteristic structural parameters such as the radius of gyration, R_g. The polystyrene samples were synthesized through anionic living chain polymerization technique using *n*-butyllithium as an initiator and methanol termination (*n*-butyl and proton terminal groups). The PS samples under study are summarized in Table 1.

Polymer samples for SFM experiments were cast from chloroform or toluene (Aldrich) solutions to form 1 to 10 μm thick films. Even ultrathin spin-coated films may still contain a considerable amount of the solvent.[29] Since the presence of even small residual concentration of the solvent can have a large influence on the measured T_g, we annealed our samples for 10 h at 110 °C, a period longer than the time over which the force−distance measurements stabilized due to solvent removal. With this annealing treatment, no spinodal dewetting of the substrate was observed.

In addition, we prepared ultrathin film samples both by spin-coating and by Langmuir−Blodgett (LB) technique. In the former case the thickness of final film on a silicon or glass substrate was controlled by choice of solution concentration (2−20 g L^{-1}) and rotation speed (1000−5000 rpm) and measured with SFM by artificially produced scratches. We prepared uniform smooth films with thickness down to 20 nm in such way. LB films were produced using a very dilute PS solution, to form a monolayer of globular-type monochain spheres at a water surface which were then transferred to a solid substrate (silicon, glass, or polymer-coated glass) for further study.[30]

Results and Discussion

Surface Glass Transition Measurements. SFM was originally developed for imaging surface topography on the atomic scale, but it also provides a sensitive tool to study surface elastic and adhesion properties.[21,22] In this context "surface" includes the thickness of the surface layer over which the property of interest (here, the surface glass transition temperature T_{g0}) is well-defined. To directly access mechanical properties on a sample surface, the SFM can be used in a nonimaging force−distance mode to perform nanoscale indentation studies. Instead of scanning laterally across the sample, the SFM tip is positioned above the area of interest on the sample and moved vertically. The tip deflection as a result of interaction with the sample surface can be then measured with an optical lever detection system. The force is determined from this cantilever deflection, and the nonlinear force−distance relation of the contact is to some extent masked by the relatively large compliance of the cantilever. Nevertheless, changes in the stiffness of the sample surface can be deduced from changes in the slope of the force−distance curve.[25] This force is plotted as a function of the motion of the piezoelectric scanner supporting the sample relative to the cantilever holder to produce a force−distance curve. Using SFM in this way provides a remarkably direct experimental method for studying surface mechanical and adhesion properties. The depth that is sampled in scanning probe techniques requires careful consideration. In purely Hertzian indentation, the depth that is elastically deformed is often taken to be several times the diameter of the contact area. Even for small tip indentations used here (2−3 nm), the thickness of the polymer sampled may be several radii of gyration. However, in the presence of viscoelastic adhesion, there will be significant irreversible effects from the peeling of the surface from the probe, and these may be localized over depth that may be small compared with the contact radius. For measurements that depend on the lateral motion of the tip,[10,14,20] this peeling contribution can be theoretically analyzed.[31] In experiments where contact between the surface and the probe is made and then broken, which is what we do, we expect viscoelastic peeling to dominate the force−distance hysteresis that is observed above T_g, with two consequences: first, that the depth of material dominating the measurements may be restricted to a few nanometers and, second, that within this volume the deformation rates may be significantly higher than in the more extended region of Hertzian deformation.

Representative force−distance curves observed for PS samples with different M_n are shown in Figure 1. At room temperature the curves take the same form as those of the glass substrate. The retraction part of force−distance curve is indistinguishable from the approach part of the curve. The main features of the curves at elevated temperatures are (i) the slope becomes less steep over the whole cycle, indicating a reduction in stiffness; (ii) the slope for retraction is steeper than for approach, creating hysteresis in the complete curve; and (iii) there is pronounced adhesion (negative force) just before separation. The appearance of the hysteresis coincides in temperature with development of an adhesion minimum on the curves and the reduction in slope of the contracting curve (corresponding to reduction of the effective stiffness of tip−surface contact). All the above effects are associated with the onset of T_g. Such behavior is not observed for the uncoated glass substrate. The three effects originate in the variation of the complex valued viscoelastic modulus ($E^* = E' + iE''$) around the glass transition temperature. Associated with the drop in the real parts (E') of the elastic stiffness tensor elements there is a peak in the imaginary parts (E''), corresponding to maximum viscoelastic loss. Below T_g, the deformation of the sample is purely elastic ($E'' = 0$), and no noticeable approach−retraction hysteresis is observed. Above and around T_g the deformed surface displays a more complex viscoelastic behavior ($E'' \neq 0$), leading to the observed strong hysteresis in loading−unloading curves. The effect is augmented by dynamic adhesion processes.[32] The strains at the edge of the contact area can be very large, and so when the contact area changes, the strain rates can be large, too. This leads to a diminished effective adhesion energy during approach and to higher adhesion energy during retraction, an effect that has long been known in the dynamic adhesion of rough surfaces to viscoelastic solids.[33]

The graphs in Figure 1 present a suite of force−distance curves at various temperatures for a series of successively higher molecular masses: (a) 3.9K, (b) 347K, and (c) 1340K. The displacement axis records the position of the cantilever tip (i.e., not the distance between the tip and the surface immediately below it) where a positive displacement corresponds to a movement away from the sample, and a negative displacement corresponds to movement of the tip into the sample. Each of the curves plotted is the average of several curves that were measured after reproducible behavior had been established. Where there is hysteresis, the upper part of the hysteresis curve corresponds to approach and the lower part to retraction. We observe differences in the nature of the hysteresis above the glass transition temperature. At high molecular weight (a good example is (c) 130 °C), contact is maintained on retraction beyond the tip height at which contact occurs during approach. At low molecular weight (an example is (a) 70 °C) it is the other way round; during approach contact is established at a point higher than where it is lost during retraction. A plausible, albeit unproven, interpretation can be given in terms of a reversal of the relative roles of bulk viscoelasticity and peeling viscoelasticity,[32] which is illustrated by the cartoons in

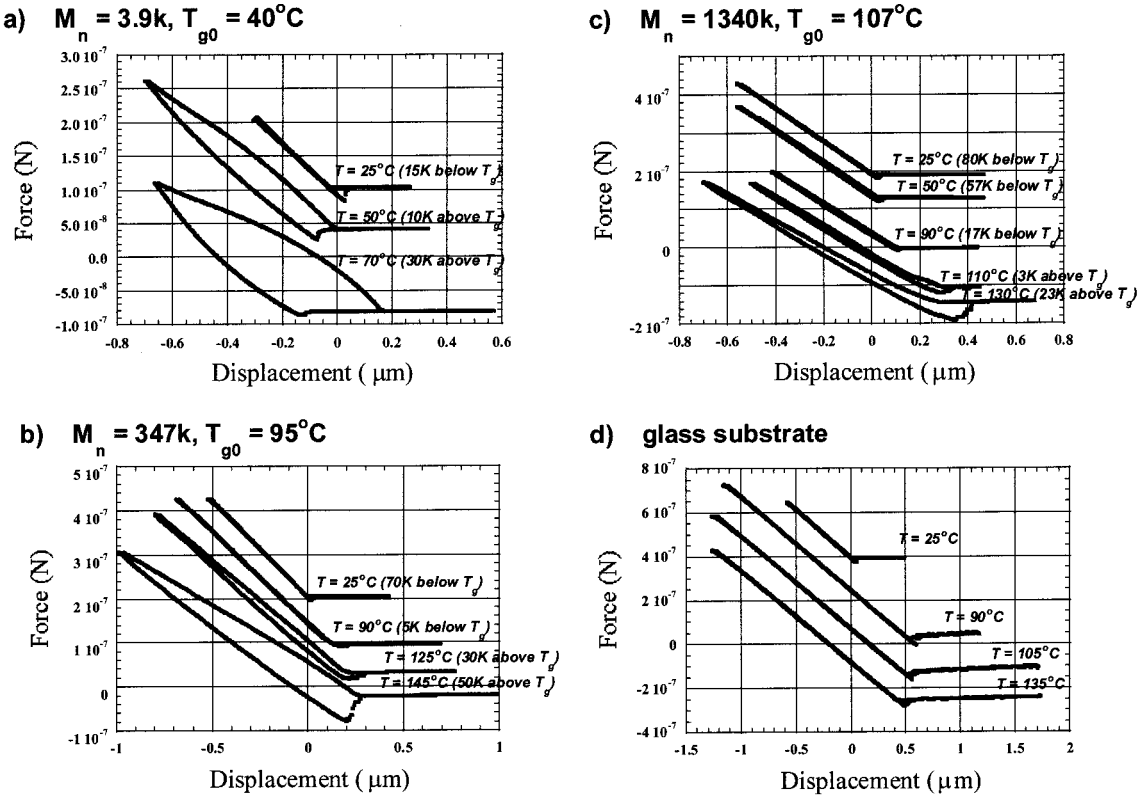

Figure 1. Examples of force−distance curves obtained at different temperatures for PS samples of molecular mass: (a) 3.9K, (b) 347K, (c) 1340K, and (d) the glass substrate. The curves are shifted vertically for clarity. The hysteresis of the downward−upward movement of the cantilever is observed for all PS samples above their glass transition points and is more pronounced for lower molecular mass compounds. No such hysteresis is detected in force−distance curves for the glass substrate at any temperature or for any of PS sample at temperatures below T_g.

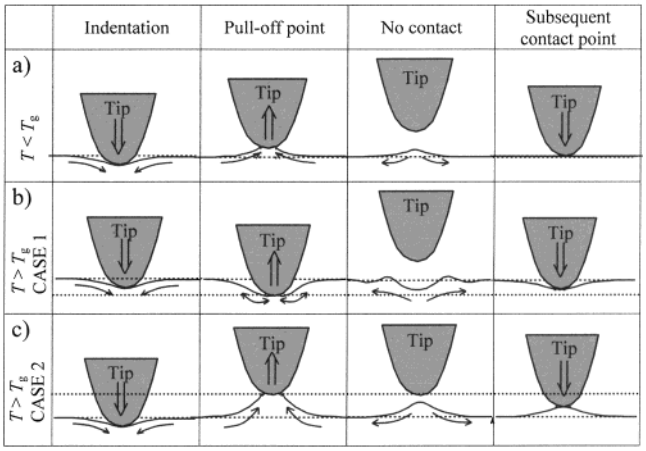

Figure 2. Mechanical interpretation of the hysteresis behavior observed for different molecular weight materials. (a) Elastic behavior at temperatures below T_g. (b) The case for low molecular weights, in which Hertzian indentation dominates and the tip restores contact with the surface at a point higher than the point at which it detaches (indicated by the fine dotted line). (c) The case observed for higher molecular weights in which the behavior can be modeled as a JKR extension to Hertzian behavior (surface viscoelastic peeling dominates), and the tip restores contact with the surface at a point lower than the point at which it detaches.

Figure 2. Figure 2a shows the elastic case, observed for all molecular weights below T_g. Figure 2b (case 1) corresponds to the situation at temperatures above T_g in which viscoelastic hysteresis in the region of strain associated with Hertzian indentation dominates. Approach proceeds qualitatively as might be expected from Hertzian contact, with a viscoelastic enhancement to the elastic stiffness. During retraction, however, viscoelasticity can prevent the polymer surface from keeping up with the indentor, and contact is lost at some displacement below the datum corresponding to the original surface height of the polymer. As retraction proceeds further, the dimple in the polymer surface relaxes toward the datum, and so during the next approach contact is established at a higher probe displacement than that at which it was lost. This process would correspond to the low molecular weight measurements such as T = 70 °C in Figure 1a. Figure 2c (case 2) corresponds to the situation at temperatures above T_g in which hysteresis in the adhesion dominates, so that the peeling energy is many times greater than the thermodynamic surface energy. The approach is similar to case 1, except that surface energy effects are diminished. During retraction, however, the energy required to peel apart the surfaces more than overcomes any reluctance of the bulk to deform, and the surface is pulled out to an extent corresponding to the unbalanced adhesion energy.[34] Once contact is lost, the resulting bump in the surface relaxes downward toward the datum, so that during the next approach contact occurs at a lower probe displacement than that at which it was lost. This process would correspond to the high molecular weight measurements such as T = 130 °C in Figure 1c. The difference in behavior with molecular weight results from the different relaxation times of the material at a given temperature. If our interpretation is correct, then these observations may give new insight into the relation between near-surface viscoelastic effects over different length scales. Although we recognize

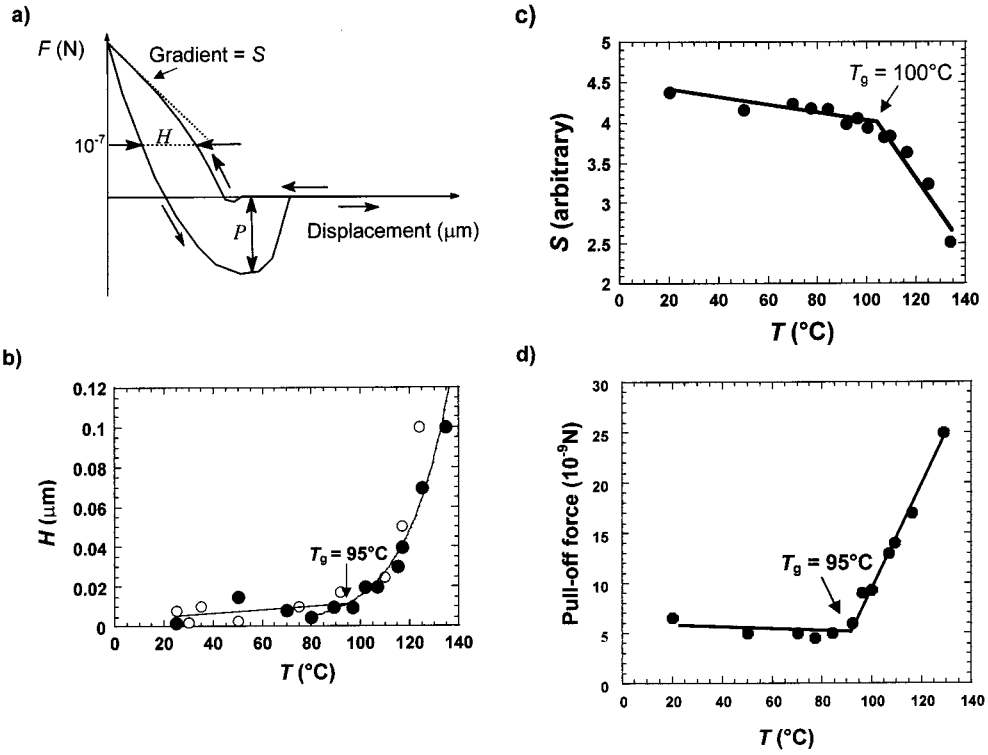

Figure 3. (a) Schematic representation of a typical force−distance curve, illustrating the three parameters that may be derived for surface glass transition estimation. Each of the parameters (b) H, (c) S, and (d) P, plotted as a function of temperature for one molecular weight (347K). The filled circles correspond to measurements taken as the sample temperature is increased in stages, and the open circles correspond to those measurements taken during cooling. The data shown in Figure 1b show example force−distance curves for this molecular weight measured during a heating run.

that the relative importance of the two effects is molecular weight dependent, we prefer not to speculate further at this point on this topic without further data and direct observations which are outside the scope of this paper. We are encouraged, however, that we deduce the same variation of the T_g from three different ways of analyzing the force−distance curves.

We determined the surface glass transition temperature (the onset of dynamical processes) from the temperature dependencies of three different parameters: the slope of the left-hand part of the curve during approach, the range of approaching−withdrawing hysteresis, and from a "pull-off force" (the adhesion interaction minimum on the force−distance curves). In Figure 3 we show how the surface glass transition temperature T_{g0} can be independently determined from each of these three phenomena. Figure 3a schematically illustrates how each of the three parameters is derived from a force−distance measurement. (i) The stiffness (S) of the sample is probed from the final gradient of the approach curve. This is related, but not equal to, the modulus of the sample. The values on the graph are derived directly from the gradient of the curve, but the absolute values of the stiffness also depend on the stiffness of the cantilever. (ii) A measure of the hysteresis (H) of the cycle is taken from the difference in displacement of the tip on the approach and retraction at an arbitrary force of 1×10^{-7} N for all cycles. (iii) The pull-off force (P) is the difference in the force between the noncontacting state and the minimum in the force as the tip is pulled away from the sample surface. Each of these parameters is plotted as a function of temperature, and by inspection we obtain a first estimate of T_{g0}. In each graph we then perform a separate linear regression of the points above and below that temperature (except for the hysteresis above T_{g0}, where an exponential fit proves to be more useful). This gives us six independently fitted lines or curves, for each of which we calculate the root-mean-square regression coefficient R_R. By repeating the process with different estimated T_{g0}, we can find the value that yields the greatest R_R. For each of the three parameters we deduce a value of T_{g0} from the intercept, and then we take their mean.

The Dependence of T_g on Film Thickness. In accordance with the data by Keddie et al.,[5] the dependence of T_g of a film with its thickness h can be described with an empirical equation:

$$T_g = T_g^{\infty}\left[1 - \left(\frac{d}{h}\right)^{\delta}\right] \qquad (1)$$

where parameters δ and d represent the strength of film−surface interaction and the depth of the correlated near-interface polymer layer, respectively. Depending on the system studied (i.e., the polymer film substrate interaction strength), these parameters were found in the range 2−5 nm for d and either 1.8 or 0.8 for δ.[5−7,34] The magnitude of the reduction of T_g for thin films depends on the strength of polymer−substrate interactions. In the case of very strong interactions of highly contracted confined polymer chains, for example hydrophilic PMMA on a hydrophilic SiO_2 surface,[6,7] the effect has even been reversed, showing a T_g increase for lower thickness.

Figure 4 shows our measurements of the thickness dependence of T_g for ultrathin spin-coated PS films of M_n = 116K. First of all, it can be concluded from the

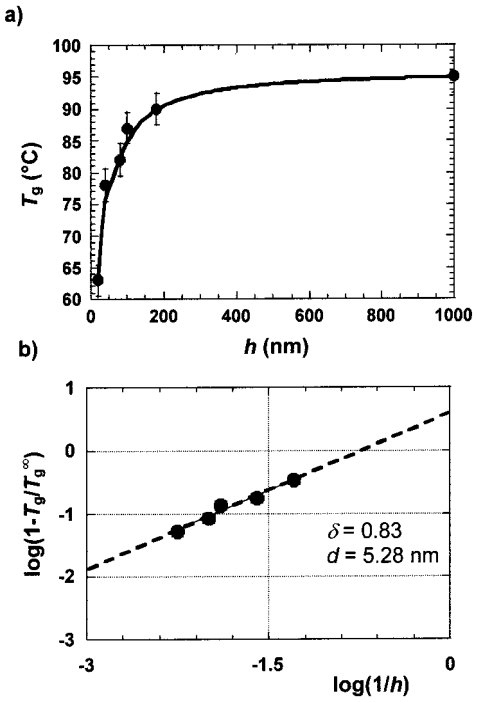

Figure 4. Depression of the glass transition with the thickness of supported films deposited on a glass substrate. The measurements were taken on a polymer of $M_n = 116$K. (b) The best fit achieved with eq 1.

figure that the surface glass transition measured in our experiments does depend on the film thickness. Second, as indicated in the inset, our data can be fitted perfectly with eq 1, giving the values of fitting parameters 5.4 and 0.83 for d and δ, respectively. The data shown in Figure 4 are therefore in good agreement with those previously reported using other techniques. Note that measurements taken of the dependence of T_g on M_n were on relatively thick films ($h > 1000$ nm) in the region where the T_g is not greatly dependent on the total film thickness. This, coupled with the inherently surface-specific nature of the measurement technique, means that substrate effects for the molecular weight dependency measurements reported here can be ignored.

Molecular Weight Dependence of T_g. The values of T_{g0} obtained for different PS fractions in our experiments are summarized in Figure 5. For comparison, in the same figure the bulk T_g is plotted as a function of molecular weight calculated from a Fox−Flory relation:[35]

$$T_g = T_g^\infty - \frac{K}{M_n} \tag{2}$$

with the infinity molecular mass glass transition temperature T_g^∞ and an empirical constant parameter K taken as 100 °C and 1.2×10^5, respectively.[3] There is a very good correlation between the bulk T_g and the surface T_{g0} values at high molecular weights, but for $M_n < 30\,000$, T_{g0} decreases faster than T_g with decreasing M_n.

The relationship in eq 2 is usually physically interpreted in terms of an increase of the free volume in a polymer material with decreasing molecular weight. There are two basic approaches to a theoretical description of the polymer surface anomalies. One of them considers the chain ends as the major factor responsible for the changes of the specific free volume and therefore influencing polymer chain mobility near the surface. An alternative approach considers a nonsymmetrical polymer segment distribution within a characteristic layer near the surface, where labile entanglements[36] are "undercompensated" from one side. This leads to different cooperative dynamics for the surface characterized with a greater correlation length.

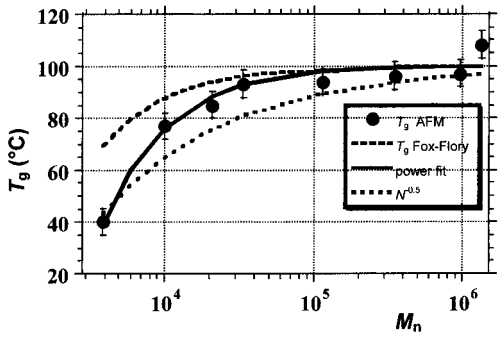

Figure 5. Surface glass transition temperatures as determined by SFM experiments vs M_n. The lines show theoretical predictions for the bulk T_g by application of Fox−Flory equation (broken line) with literature coefficients, $N^{-0.5}$ scaling low predicted for the localization of the chain ends on the surface (dotted line), again, using literature coefficients for the bulk material, and the best power-law fit of our data set achieved by an application of eq 6 (solid line).

Unlike other glass-forming materials, polymers have intrinsic impurities: the polymer chain ends. As a result, polymer materials may have molecular mass depression of T_g, which is associated with the polymer chain ends for smaller polymer chains. Localization of the chain ends is an important factor in the context of glass transition depression as a mechanism for increasing the free volume in the system. Some authors explain the enhanced polymer chain mobility as an increase of the free volume due to localization of chain ends near the surface.[10] It can be argued, however, that the chain ends fraction at the surface is too small to have so drastic impact on the free volume and thus the mobility at the polymer free surface at least for medium molecular mass PS samples studied by Keddie and Forrest.[11] Mayes[28] considered this process near a polymer free surface and suggested a new effective chain length, which would give the molecular weight equivalent for the same fraction of chain ends as in the bulk. The localization of chain ends at a polymer surface can depress T_{g0} by locally increasing the free volume. The reduction in T_{g0} then scales as $M_n^{-0.5}$ because of the Gaussian (random walk approximation) distribution of the chain segments in a polymer:

$$T_{g0} = T_g^\infty - CN^{-0.5}\frac{a}{D} \tag{3}$$

where a is the chain segment length, N is the average length of polymer chains in units of segments, D is depth of the surface layer under consideration, and C is an empirical parameter.

Alternatively, the effect of molecular mass on T_g has been discussed in the literature and generally understood for bulk polymer materials as an appearance of polymer chain entanglements.[3,4] The entanglements are responsible for polymer-like behavior such as diffusion by reptation and non-Newtonian viscosity, as opposed to low molecular mass Rouse-type behavior. They appear to play an important role for chain molecules

starting from a characteristic molecular mass M_c, which depends on the polymer type. Such behavior can be described in terms of a Fox−Flory relationship (eq 2).

The empirical coefficient K in eq 1 is related to the thermal expansion coefficients of the glass-forming material in the glass state α_G and in the melt α_M:[37,38]

$$K \sim (\alpha_M - \alpha_G)^{-1} \tag{4}$$

K will also depend (through the thermal expansion) on the characteristic molecular mass M_e, an average length of polymer chain segments between the entanglements.[5,38] It therefore describes the appearance of viscoelastic behavior. At a free polymer surface the thermal expansion may occur preferentially in the direction along the normal to the surface plane. Computer simulations also reveal an asymmetry between the motion in plane of the film and the motion out of the film plane, and the fact that the segments situated close to the free surface are more mobile than the bulk ones.[39] Consistency between ellipsometry data for supported films and Brilluoin spectroscopy measurements for free-standing films has been found by incorporation of an idea of a characteristic length scale for cooperative dynamics[16] into the simple empirical surface layer model given in eq 1. The cooperative dynamics model also suggests the existence of the surface layer with enhanced mobility due to the release of steric constraints but with slightly different functional dependence on the film thickness:

$$T_g(h) = T_g^\infty + \frac{2\xi(T_g(h))(T_g^{surf} - T_g^\infty)}{h} \tag{5}$$

where T_g^{surf} is the glass transition temperature of the near-surface region of the size $\xi(T)$. The cooperativity length ξ is then described with a power law dependence on a deviation of the actual temperature from some characteristic temperature T_c: $\xi(T) \sim \alpha(T_c - T)^\gamma$ (α and γ being empirical fit parameters). Fitting the empirical parameters in eq 5 for PS has given values for $\xi(T)$ of around few nanometers for the temperature range 275−375 K. A wide range of terms, such as "characteristic length scale of cooperative dynamics", "correlated segments", or "loops", have been used to describe liquid-like movement of several polymer segments in the surface layer comparable with the radius of gyration. These lengths will be connected with the idea of "entanglements" within the polymer which are themselves important in the consideration of the "free volume" of the system. This influence of entanglements on polymer dynamics is expected to be different for the free polymer surface. The number of entanglements per unit volume for the latter case is smaller than the bulk value due to a break in symmetry at the polymer/air interface. Such a view, albeit oversimplified, is nevertheless a useful first-approximation description of the surface glass transition behavior with the molecular weight. The entanglements should not be understood as only interchain loops. Two different types of entanglements, inter- and intramolecular, were discussed more than 25 years ago by Lipatov and co-workers.[40] Recent theoretical analysis performed by Semenov[41] predicts that the effect of molecular entanglement becomes more important near the surface for a thickness comparable to R_g.

We attempted to fit our data for the surface T_g depression by using the different theoretical models described above. These relationships are plotted as the dashed curves in Figure 5, using literature values for the infinite molecular mass glass transition temperature $T_{g0}^\infty = 100$ °C and the empirical parameters $C = K = 1.2 \times 10^5$.[3] The reduction in T_g becomes significant below a characteristic molecular mass M_c that depends on the polymer type: previous bulk experiments suggest $M_c = 19\,500$[28] for PS. In Figure 5 the first significant departure of our experimental data from T_g^∞ occurs for $M_n = 22\,000$, which is not too different.

As is apparent from Figure 5, neither of these theoretical models using literature values of C, K, and T_{g0}^∞ gives a satisfactory fit to our data. We therefore investigated what parameters would give a best power law fit to a curve:

$$T_{g0} = T_{g0}^\infty - KM_n^m \tag{6}$$

which yielded the parameters $T_{g0}^\infty = 96.9 \pm 0.3$, $m = -1.06 \pm 0.05$, and $K = (4.3 \pm 2.0) \times 10^5$. The value for m, being close to −1, rather than −0.5, points unequivocally toward an explanation of the T_{g0} depression in terms of entanglement of chains rather than in terms of localization of chain ends at the surface.

The power law fit revealed a value of K that is considerably higher for the surface in comparison to the bulk state of PS fractions. Anisotropy of chain mobility at the polymer surface[39] predicts a change in the thermal expansion at the glass transition that is 1.75 times smaller for the surface than the bulk. Additionally, there is half the average number of entanglements at the surface because only one of two hemispheres is available for loops in the molecular chain. A combination of these two factors predicts a value of the K coefficient that is 3.5 times higher for the surface than the bulk (i.e., $1.2 \times 10^5 \times 1.75 \times 2 = 4.2 \times 10^5$). This predicted value is very close to the one found from our power law fit. Our experiments therefore support an entanglement and cooperative dynamic T_g reduction description rather than a description relying on the chain-end localization model. Our data support the theoretical predictions and may also provide useful comparison with direct measurements by scanning thermal expansion microscopy.[42]

Langmuir−Blodgett Layers. Experiments performed with PS Langmuir−Blodgett (LB) films further support our earlier conclusion of the crucial role of entanglements in additional surface free volume creation. As illustrated in Figure 6a, a monolayer of PS molecules applied using LB techniques adds a considerable amount of additional free volume when deposited on top of a glassy PS surface due to lack of entanglements between the polymer chains. We used relatively thick PS spin-coated film, such that the surface glass transition temperature of this film is that of the surface of a bulk material. However, deposition of a single additional LB layer of polymer chains reduces the glass transition on the surface by 12 K. Because of the glassy state of the surface of the PS spin-coated film substrate ($T_g = 95$ °C for this molecular weight fraction), the molecules in the LB layer cannot escape from the surface into the underlying film, as would be thermodynamically advantageous, unless the system is heated above the substrate glass transition temperature. This migration of the chains into the bulk can be observed, however, after several measurements during which the

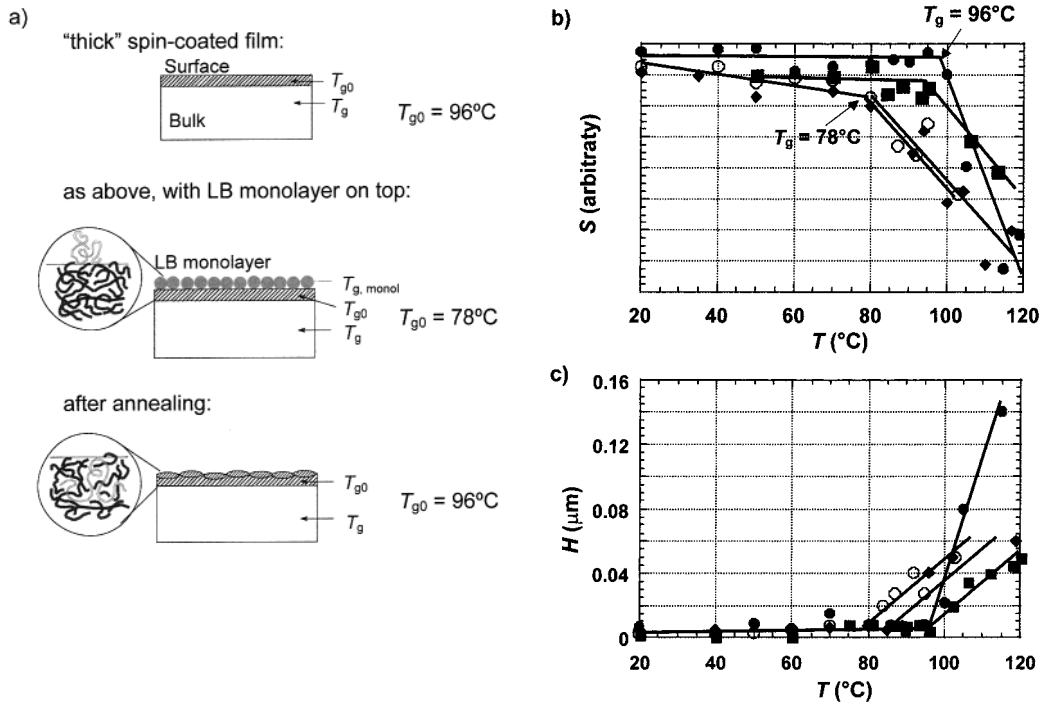

Figure 6. (a) Schematic illustration of a Langmuir−Blodgett monolayer on a spin-coated thick PS film indicating structural changes from the individual self-entangled state for polymer chains in the Langmuir monolayer to intermoleculary entangled ("normal") structure achieved within several temperature scans as a result of annealing. Local glass transition temperatures corresponding to individual polymer chains of Langmuir monolayer $T_{g,monol}$, surface layer of the polymer substrate T_{g0}, and bulk T_g are indicated and the effective measured values of T_{g0} are given. Experimentally measured parameters (b) S and (c) H derived from the force−distance measurements for successive heating−cooling cycles during which the polymer is raised in temperature above its T_g. Solid circles correspond to measurements taken during the first heating cycle from the thick spin-coated PS substrate, open circles for the first heating cycle on the LB monolayer on top of the substrate, diamonds the properties measured during the second heating cycle on the LB sample, and squares from the third heating cycle.

material is heated above its T_g. This is shown in Figure 6b,c where two parameters (stiffness and hysteresis) from the force−distance curve are plotted for successive heating cycles. The pull-off force curves give inconclusive results in this case, probably due to the irregular topography of the surface. For each cycle, the measured surface T_g increases until it reaches the value for the conventionally spin-cast polymer film. At this point, the molecules from the LB layer have become intermolecularly entangled and incorporated into the underlying film. As presented in surface structure scheme (Figure 6a), the contribution of the chain ends into free volume of the sample surface is constant in this particular configuration. However, the entanglement density and therefore the free volume at the surface are changing during the annealing procedure because of polymer chain interdiffusion. In our force microscopy experiments we measure mechanical characteristics of polymer single-chain spheres together with the near-surface layer comparable with PS globular diameter (10 nm for this molecular weight), thus probing the changes of the free volume of the system. Figure 7 presents atomic force microscopy images of the LB layer (a) before heating and after (b) two and (c) three heating cycles. The smoothing of the topography observed is consistent with the molecules of the LB layer becoming incorporated over a period of time into the underlying substrate. These measurements add further weight to the conclusion that the entanglements, and in particular the interchain entanglements, rather than chain-end segregation play an important role in the repression of the T_g at the surface.

Conclusions

A simple and reliable technique for measuring the surface glass transition (and other stress relaxation phase transitions) based on analysis of SFM force−distance curves has been suggested and successfully tested for a set of polystyrenes with molecular mass ranging from 3.9×10^3 to 1.34×10^6 g mol^{-1}.

The values of the surface glass transition for the samples with $M_n > 30\,000$ have been found to be the same as the corresponding bulk values. However, low molecular mass polymers behave differently. Our experiments support the depression of the glass transition at the polymer surface observed previously. The magnitude of this depression increases with decreasing molecular mass for low molecular mass fractions of PS. The molecular mass dependence of T_g correlates with the structural and dynamical parameters of polymer chains: the presence of a virtual network of labile entanglements. Fitting a power-law expression for the dependence of surface T_g on M_n showed an good fit with an exponential factor close to −1, i.e., in agreement with Fox−Flory scaling. The preexponential coefficient is about 3.5 times greater than for the bulk value. This can be related to the predicted decrease in the number of entanglements in the surface layer.

For very thin films the depression of the T_g that has been previously observed for very thin layers has been confirmed here.

Observation of the diffusion of molecules from a Langmuir−Blodgett monolayer deposited on a PS substrate provides additional evidence that molecular

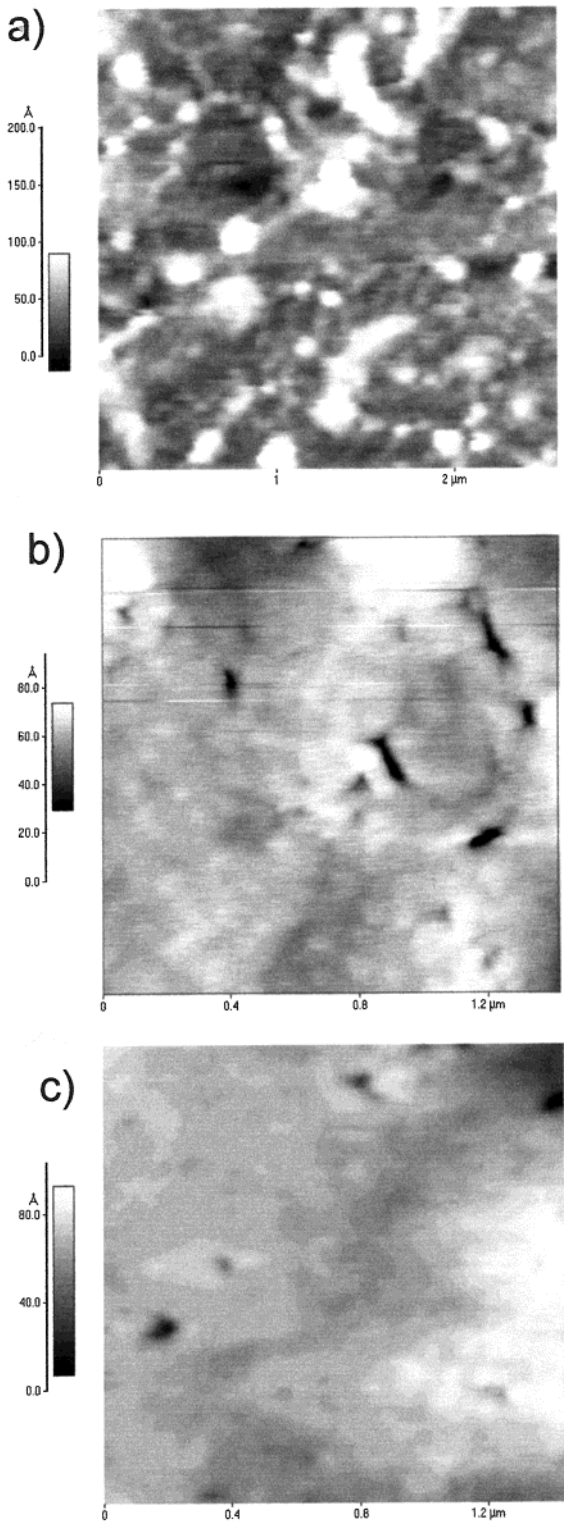

Figure 7. Atomic force microscopy images of PS 116K LB monolayer film on top of relatively thick spin-cast film of the same polymer. (a) After initial deposition the surface has a rough, granular morphology. After (b) two and (c) three temperature scans from 25 to 150 °C, the surface smoothes out as the LB monolayer is incorporated into the substrate polymer layer.

entanglement rather than chain-end segregation effects are responsible for the depression of T_g at the surface.

Acknowledgment. The authors thank Dr. Z. Kazantseva (Institute of Semiconductor Physics, Kiev, Ukraine) for her help with PS LB films preparation, Professor K. L. Johnson FRS, FREng (University of Cambridge, U.K.), for useful comments on the contact mechanics, Professor Y. Lipatov and Professor V. Privalko (Institute of Macromolecular Chemistry, Kiev, Ukraine) for fruitful discussions, and Dr. Y. Tsukahara and the Toppan Printing Co. for intellectual and financial support for this research.

References and Notes

(1) Salaneck, W. R.; Bredas, J. L. *MRS Bull.* **1997**, *22*, 46−51.
(2) Deng, C.-S.; Assender, H. E.; Dinelli, F.; Kolosov, O. V.; Briggs, G. A. D.; Miyamoto, T.; Tsukahara, Y. *J. Polym. Sci., Part B: Polym. Phys.* **2000**, *38*, 3151−3162.
(3) Sperling, L. H. *Introduction to Physical Polymer Science*; John Wiley & Sons: New York, 1992.
(4) Rodrigez, F. *Principles of Polymer Systems*; Taylor & Francis: Washington, DC, 1996.
(5) Keddie, J. L.; Jones, R. A. L.; Cory, R. A. *Europhys. Lett.* **1994**, *27*, 59−64.
(6) Jones R. A. L.; Richards, R. W. *Polymer at Surface and Interfaces*; Cambridge University Press: Cambridge, UK, 1999.
(7) Forrest, J. A.; Dalnoki-Veress, K.; Dutcher, J. R. *Phys. Rev. E* **1997**, *56*, 5705−5716.
(8) Forrest, J. A.; Dalnoki-Veress, K.; Dutcher, J. R. *Phys. Rev. E* **1998**, *58*, 6109−6114.
(9) Kajiyama, T.; Tanaka, K.; Takahara, A. *Macromolecules* **1997**, *30*, 280−285.
(10) Tanaka, K.; Takahara, A.; Kajiyama, T. *Macromolecules* **2000**, *33*, 7588−7593.
(11) Kerle, T.; Lin, Z.; Kim, H.-C.; Russell, T. P. *Macromolecules* **2001**, *34*, 3484−3492.
(12) Forrest J. A.; Mattsson, J. *Phys. Rev. E* **2000**, *61*, R53−R56.
(13) Liu, Y.; Russell, T. P.; Samant, M. G.; Stöhr, J.; Brown, H. R.; Cossy-Favre, A.; Diaz, J. *Macromolecules* **1997**, *30*, 7768−7771.
(14) Ge, S.; Pu, Y.; Zhang, W.; Rafailovich, M.; Sokolov, J.; Buenviaje, C.; Buckmaster, R.; Overney, R. M. *Phys. Rev. Lett.* **2000**, *85*, 2340−2343.
(15) Bliznyuk, V. N.; Assender, H. E.; Briggs, G. A. D. Submitted.
(16) Mattsson, J.; Forrest, J. A.; Börjesson, L. *Phys. Rev. E* **2000**, *62*, 5187−5200.
(17) Fukao, K.; Miyamoto, Y. *Europhys. Lett.* **1999**, *46*, 649−654.
(18) Fukao, K.; Miyamoto, Y. *Phys. Rev. E* **2000**, *61*, 1743−1754.
(19) De Gennes, P. G. *Eur. Phys. J. E* **2000**, *2*, 201−203.
(20) Dinelli, F.; Buenviaje, C.; Overney, R. M. *J. Chem. Phys.* **2000**, *113*, 2043−2048.
(21) Yamanaka, K.; Ogiso, H.; Kolosov, O. *Jpn. J. Appl. Phys.* **1994**, *33*, 3197−3203.
(22) *Scanning Probe Microscopy of Polymers*; Ratner, B. D., Tsukruk, V. V., Eds.; ACS Symposium Series 694; American Chemical Society: Washington, DC, 1998.
(23) Hammiche, A.; Pollock, H. M.; Hourston, D. J.; Reading, M.; Song, M. *J. Vac. Sci. Technol.* **1996**, *B14*, 1486−1491. Pollock, H. M.; Hammiche, A.; Song, M.; Hourston, D. J.; Reading, M. *J. Adhes.* **1998**, *67*, 217−223.
(24) Young's modulus can be estimated from force−distance curves as an inclination of the linear part of the curve corresponding to intimate contact between the SFM tip and the polymer surface.[26] This approach is valid in the case of a linear Hooke's law approximation, which is true for the small tip indentations typical for SFM experiments. As it has been pointed out,[27] if the cantilever's effective spring constant is smaller than the elastic modulus of the surface, the force−distance measurement will probe primarily the cantilever stiffness. Drastic changes in surface Young's modulus and adhesion properties are expected in a vicinity of T_g. Therefore, a more flexible cantilever may become stiffer than the surface above its glass transition. We have used cantilevers with the stiffness 0.26−0.40 N/m in our experiments, which typically apply a pressure of about 10−100 MPa. Such pressure will only slightly indent the glassy polymer, without unduly deforming it above the T_g.[3]
(25) Tsukruk, V. V.; Huang, Z.; Chizhik, S. A.; Gorbunov, V. V. *J. Mater. Sci.* **1998**, *33*, 4905−4909.
(26) Burnham, N. A.; Gremaud, G.; Kulik, A. J.; Gallo, P.-J.; Oulevey, F. *J. Vac. Sci. Technol. B* **1996**, *14*, 1308−1312.
(27) Bliznyuk, V. N.; Kolosov, O. V.; Assender, H. E.; Briggs, G. A. D. Manuscript in preparation.

(28) Mayes, A. M. *Macromolecules* **1994**, *27*, 3114−3115.
(29) Frank, C. W.; Rao, V.; Despotopoulou, M. M.; Pease, R. F. W.; Hinsberg, W. D.; Miller, R. D.; Rabolt, J. F. *Science* **1996**, *273*, 912−915.
(30) Kumaki, J. *Macromolecules* **1988**, *21*, 749−755.
(31) Savkoor, A. R.; Briggs, G. A. D. *Proc. R. Soc. London A* **1977**, *356*, 103−114.
(32) Johnson, K. L. *ACS Symp. Ser.* **1999**, *741*, 24.
(33) Briggs, G. A. D.; Briscoe, B. J. *Nature (London)* **1976**, *260*, 313−315.
(34) Prucker, O.; Christian, S.; Bock, H.; Ruhe, J.; Frank C. W.; Knoll, W. *Macromol. Chem. Phys.* **1998**, *199*, 1435−1444.
(35) Fox T.; Flory, P. *J. Polym. Sci.* **1954**, *14*, 315.
(36) Wu, D. T.; Fredrickson, G. H.; Carton, J.-P.; Ajdari, A.; Leibler, L. *J. Polym. Sci., Polym. Phys. Ed.* **1995**, *33*, 2373−2389.
(37) *Polymers in Solutions: Theoretical Considerations and Newer Methods of Characterization*; Forsman, W. C., Ed.; Plenum Press: New York, 1986.
(38) De Gennes, P.-G. In *Physics of Polymer Surfaces and Interfaces*; Sanchez, I. C., Ed.; Butterworth-Heinemann: Boston, 1992.
(39) Mansfield, K. F.; Theodorou, D. N. *Macromolecules* **1991**, *24*, 6283−6294.
(40) Privalko, V. P.; Lipatov, Yu. S. *Makromol. Chem.* **1974**, *175*, 641−654.
(41) Semenov, A. N. *Phys. Rev. Lett.* **1998**, *80*, 1908−1911.
(42) Hammiche, A.; Price, D. M.; Dupas, E.; Mills, G.; Kulik, A.; Reading, M.; Weaver, J. M. R.; Pollock, H. M. *J. Microsc.* **2000**, *199*, 180−190.

MA011326A